



Published in final edited form as:

Chem Mater. 2020 March 10; 32(5): 2070–2077. doi:10.1021/acs.chemmater.9b05164.

Influence of Lithium Polysulfide Clustering on the Kinetics of Electrochemical Conversion in Lithium-Sulfur Batteries

Abhay Gupta[†], Amruth Bhargav[†], John-Paul Jones[‡], Ratnakumar V. Bugga[‡], Arumugam Manthiram^{†,*}

[†]Materials Science & Engineering Program and Texas Materials Institute, The University of Texas at Austin, Austin, TX 78712, USA

[‡]Jet Propulsion Laboratory, California Institute of Technology, Pasadena, CA 91109, USA

Abstract

The electrochemistry of lithium-sulfur (Li-S) batteries is heavily reliant on the structure and dynamics of lithium polysulfides, which dissolve into the liquid electrolyte and mediate the electrochemical conversion process during operation. This behavior is considerably distinct from the widely used lithium-ion batteries, necessitating new mechanistic insights to fully understand the electrochemical phenomena. Testing at low-temperature conditions presents a unique opportunity to glean new insights into the chemistry in kinetically constrained environments. Under such conditions, despite the low freezing point and favorable ionic conductivity of the glyme-based electrolyte, Li-S batteries exhibit counterintuitively poor performance. Here, we show that beyond just existing in single-molecule conformations, lithium polysulfides tend to cluster and aggregate in solution, particularly at low-temperature conditions, which subsequently constrains the kinetics of electrochemical conversion. Energetics and coordination implications of this behavior are extended towards a new framework for understanding the solution-coordination dynamics of dissolved lithium species. Based off this framework, a favorable strongly-bound lithium salt is introduced in the Li-S electrolyte to disrupt polysulfide clustered networks, enabling substantially enhanced low-temperature electrochemical performance. More broadly, this mechanistic insight heightens our understanding of polysulfide chemistry irrespective of temperature, confirming the link between the solution conformation of active material and electrochemical behavior.

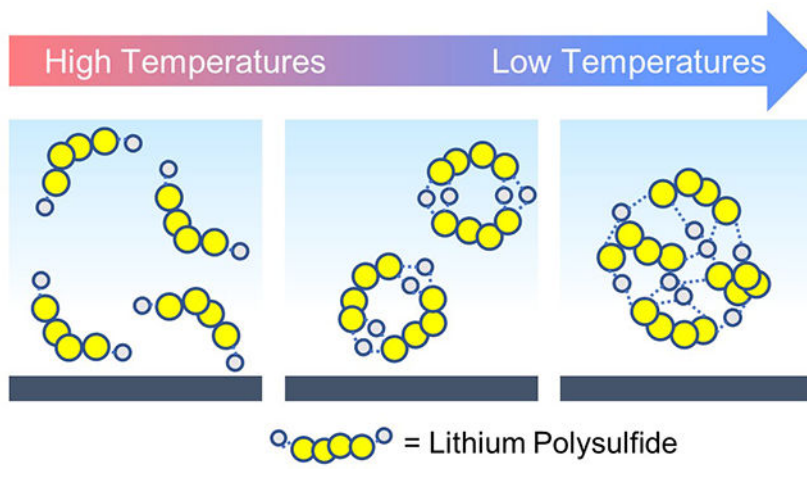
Graphical Abstract

*Corresponding author: manth@austin.utexas.edu (A. Manthiram).

The authors declare no competing financial interests.

Supporting Information

Additional supporting information is available free of charge at the ACS Publications Website. This includes: additional experimental methodology, supplemental physical and spectroscopic data on polysulfides at low temperatures, additional NMR data, additional analysis and accompanying discussion of FTIR data, an analysis of clustering phenomena variation with temperature, variable temperature cycling data, coordinates of all computational structures used in this work with calculated energies, and partial charge analysis of Li₂S₄ clusters.



Introduction

Lithium-sulfur (Li-S) batteries have the potential to transform the energy storage landscape owing to their high theoretical specific energy of $2,600 \text{ Wh kg}^{-1}$. This high gravimetric energy capability is particularly appealing for use-cases, such as unmanned aerial vehicles, electric vehicles, and missions in space, as these applications all benefit greatly from the minimization of mass.¹ However, an additional constraint these applications share is their recurring exposure to low-temperature or, in the case of space applications, extremely low-temperature environments.^{2,3} Developing reliable energy storage with both high specific energy and greater low-temperature operational capability will be imperative as humanity continues navigating harsh environments on Earth and ventures further into the outer solar system.⁴ The Li-S chemistry presents an excellent platform upon which to develop a next generation, energy-dense battery with increased low-temperature capability. Furthermore, evaluation of the Li-S battery at low temperatures can present a unique opportunity to investigate the polysulfide chemistry at kinetically limiting conditions, providing new insights into the intricate chemical system.

Low-temperature conditions present severe challenges for traditional lithium-ion batteries. Limited thermal kinetic energy hinders diffusion of lithium ions through the electrolyte-electrode interfaces and bulk of the electrodes, and can even induce freezing in standard carbonate-based electrolytes.⁵⁻⁷ Largely for this reason, commercial lithium-ion batteries generally cannot be used below -20°C .⁷ In contrast, the predominantly used electrolyte solvents in Li-S batteries, 1,3-dioxolane and 1,2-dimethoxyethane (DOL:DME, 1:1 by volume), have very low freezing points of -95 and -58°C , respectively.⁸ These low freezing point solvents would be expected to enable outstanding low-temperature performance in Li-S batteries. However, Li-S batteries also experience significantly curtailed performance at low temperatures,⁹⁻¹¹ presenting a large barrier to implementation in the aforementioned applications of interest.¹²

The presence of soluble lithium polysulfides (Li_2S_x , $2 < x < 8$) in the electrolyte provides an additional degree of complexity when contending with capacity-loss mechanisms at low

temperatures. The initial S₈ elemental solid and the final reaction products, insoluble Li₂S and Li₂S₂, are highly electrically and ionically insulating, presenting large barriers to electron flow and subsequent electrochemical reactions. Therefore, Li-S discharge relies on solution-mediated reduction through the generation of soluble polysulfides, which can enable facile charge transfer in solution.^{13–16} Thus, understanding the unique nature of Li-S reaction chemistry at low temperatures requires mechanistic insights that are fundamentally different than those for traditional battery chemistries, as the physical and chemical properties of the electrolyte and active material are interdependent and cannot be decoupled.^{17–20} This calls for further research into the mechanisms behind the low-temperature behavior of Li-S batteries.

In this work, we investigate and explore the Li-S battery chemistry through a suite of experimental and computational tools. Through this, we unveil a new mechanism that explains the battery's nonintuitive electrochemical behavior at low temperatures, polysulfide clustering. Given the poor material utilizations seen in the broader Li-S literature (~60% of theoretical), a detailed understanding of this mechanism also provides significant insight into room-temperature behavior.²¹ We build upon this understanding by outlining new design principles for Li-S batteries to counteract the detrimental mechanisms displayed at low-temperature conditions.

Experimental Section

Conductivity Measurements:

The ionic conductivity of the electrolyte consisting of 1 M LiTFSI and 0.2 M LiNO₃ in DOL:DME (1:1 by volume) was evaluated with a Fisher Scientific Accumet 2-cell conductivity cell with platinum electrodes. A cell constant of 1.0 was determined with a 0.1 M KCl in deionized water solution. Conductivities were determined from values of resistance found through AC impedance with a Biologic VMP2 potentiostat, with a scan range of 10⁶ Hz to 10 Hz and a 5 mV amplitude perturbation.

Li-S Cell Fabrication:

Li-S cells were assembled in CR-2032 type coin cells, consisting of a sulfur cathode, lithium-metal foil anode, electrolyte, and a Celgard 2325 separator. The sulfur cathode consisted of a sulfur-carbon composite with 60% sulfur content cast onto aluminum foil, with a sulfur loading of approximately 3.85 mg cm⁻². 40 uL of electrolyte was utilized for variable temperature cycling. 1 M LiTFSI and 0.2 M LiNO₃ in DOL-DME were used in all electrochemical studies except during the variable temperature cycling and where otherwise stated. Cell assembly was performed inside an argon-filled glovebox.

Electrochemical Cell Testing:

Cells were rested for 8 h at a given temperature before beginning cycling. An Arbin battery cycler was used to galvanostatically discharge cells at a rate of C/20, with 1C = 1,672 mA g⁻¹ of sulfur in the cathode. Cells were cycled between a voltage window of 2.7 and 1.7 V, except in the case of -20 and -40° C where a lower cutoff of 1.5 V was used. Temperature was controlled with an Espec SH-241 bench-top environmental chamber.

⁷Li-Nuclear Magnetic Resonance (NMR) Spectroscopic Studies:

NMR samples consisted of 0.1 M nominal Li₂S₄ in a 1:1 volume mixture of deuterated THF and DME or 0.1 M LiTFSI and 0.05 M LiNO₃ in a ternary mixture of DOL, DME, and deuterated THF (1:1:1 by volume). Each solution was prepared inside an argon-filled glovebox by adding a set amount of Li₂S and sulfur in a ratio stoichiometrically equivalent to Li₂S₄ to vials containing the solvents outlined above. 600 μL of each sample was placed in a NMR tube along with a sealed capillary tube. This capillary tube contained 0.5 M LiCl in THF and was used as an external reference without influencing the coordination state of the sample. NMR tubes were sealed in an argon filled glovebox before being brought out of the glovebox and analyzed. ⁷Li-NMR scans were performed with a Varian VNMRS 400 MHz spectrometer, and temperature was controlled at -60° C with a flow line containing liquid nitrogen. 4 scans were run at each temperature, with a relaxation delay of 60 s, a pulse width of 2 s, and an acquisition time of 4 s.

Computational Methods:

All calculations were performed with the use of Gaussian 09 Rev. A.02.²² The hybrid DFT method B3LYP was used to optimize structures and for all calculations, along with the Pople basis set 6-31+G(d,p). Input files and geometrical structures were prepared using Avogadro Version 1.2.0.²³ The influence of solvent was implicitly modelled through the use of the polarizable continuum model (PCM) using THF solvent, whose properties closely model the glyme-based solvents of interest in Li-S batteries. Free energies of formation and ionic association energies were calculated by taking the difference of each constituent ion's sum of electronic and zero-point energies (found through a vibrational frequency analysis). The stability of each optimized structure was verified by checking that the vibrational frequency analysis outputted no negative frequencies. Partial charge analysis was conducted with Natural Bond Orbital (NBO) calculations.²⁴

Results and Discussion

Low-Temperature Electrochemical Behavior:

As expected from the use of low freezing point DOL and DME solvents, the conductivity of the Li-S electrolyte remains quite high at low temperatures, particularly compared to traditional carbonate-based electrolytes.⁶ This is shown in Figure 1a. However, as shown in Figure 1b, Li-S batteries experience sizeable losses in discharge capacity even at moderately low temperatures, with capacity dropping from 960 mA h g⁻¹ at 25° C to 160 mA h g⁻¹ at -20° C.

Notably, there is a disproportionate loss in capacity in the lower voltage plateau region. The capacity in this region, which corresponds to the conversion of soluble Li₂S₄ to the insoluble Li₂S discharge product, reduces by 35% at 0° C and altogether disappears during discharge at -20° C.¹⁴ At this temperature, the conversion to Li₂S is completely inhibited, with possible nucleation overpotential extending beyond the voltage cut-off of the cell.

The performance of a Li-S battery is highly sensitive to the total amount of electrolyte in the cell, quantified by the metric electrolyte-to-sulfur (E/S) ratio (in μL_{electrolyte} mg⁻¹_{sulfur}).^{21,25}

Taking this into consideration, variations in the low-temperature behavior due to electrolyte amount was tested by comparing cells with E/S ratio ranging from 25 $\mu\text{L mg}^{-1}$ (Figure 1b) to 7.5 $\mu\text{L mg}^{-1}$ (Figure 1c). As shown, the cell with lean electrolyte significantly underperforms the cell with excess electrolyte at low temperatures, with a 3 times reduction in capacity at both 0 and -20°C . Even more so than before, there is disproportionate capacity loss stemming from the second plateau region, with this conversion being completely inhibited at 0 and -20°C .

A common link between the low-temperature electrochemistry presented thus far is the stunted behavior in the second plateau region. At the onset of this conversion process, the dominant electroactive species in solution is Li_2S_4 .²⁶ The ability of cells with excess electrolyte to better withstand the detrimental effects of low-temperature hints that the underlying cause of capacity loss relates to an interplay between Li_2S_4 and electrolyte. Apart from conductivity, other known solvent-dependent properties that could account for this, such as solubility, solution viscosity, or polysulfide speciation, do not seem to show significant enough dependencies with decreasing temperature to adequately explain this behavior (demonstrated in Supporting Information Figure S1). The Li-S battery chemistry is dictated by the active material and electrolyte being coupled together physically and chemically in solution. Taking this into consideration, a final property that may influence the solution-mediated mechanisms of the Li-S chemistry and explain this behavior is the coordination dynamics of soluble Li_2S_4 .

The coordination of dissolved species in solution can be much more complex than the commonly envisioned “free ions” distributed in solvent. Rather, with increasing concentration, ions can begin to directly interact with counter-ions through short-range electrostatic interactions, leading to a wide degree of coordination and aggregation behavior.²⁷ These states of existence can vary from solvent-separated ion-pairs and contact-ion pairs to ion aggregates, where ions are directly coordinated to increasing numbers of counter-ions in solution.²⁸

The detrimental behavior of the Li-S system at low temperatures could correspond to an increased tendency for polysulfides to form clustered aggregates in solution. As the major kinetic limiting step is the conversion of dissolved polysulfide molecules to solid precipitates, large-scale clustering of Li_2S_4 would be accompanied by the formation of strong, robust networks of $\text{Li}^+-\text{S}_4^{2-}$ linkages, restricting the ability to further convert this species to Li_2S . The notion of polysulfide clustering has been discussed in prior literature, though their possible increased existence at low temperatures has never been touched upon.^{29–32} This emergent phenomenon would simultaneously explain both the discrepancies in electrochemical behavior at low temperatures as well as the subsequent dependency with electrolyte amount, and thus merits further detailed investigation.

Energetics Consideration of Polysulfide Clustering:

Clustering and aggregation phenomena stem from the ability of ions and counter-ions in solution to electrostatically coordinate and form strong linkages and networks, minimizing the overall energy of each ion. Computational chemistry is an excellent tool with which to evaluate this behavior, as key insights on energetics can be gained from first principles.

Given that the conversion of Li_2S_4 is particularly inhibited at low temperatures, various hypothetical geometries of $(\text{Li}_2\text{S}_4)_n$ clusters ($n = 1, 2,$ and 4) were computationally evaluated using hybrid density functional theory (DFT). The formation energy of each cluster from constituent Li^+ and S_4^{2-} ions was found using Equation 1 and normalized to a $\text{kJ mol}^{-1} \text{Li}^+$ basis. These modelled geometries and their associated formation energies are displayed in Figure 2.

$$\Delta G_{\text{formation}} = \frac{1}{2n} \times [G_{(\text{Li}_2\text{S}_4)_n} - n(2G_{\text{Li}^+} + G_{\text{S}_4^{2-}})] \quad (1)$$

The various clusters were modelled by placing a chosen number of single Li_2S_4 molecules in close proximity and from there, iteratively finding the lowest energy configuration of molecules, similar to how lithium polysulfides may actually aggregate and coalesce in solution in a Li-S battery. Due to electrostatic interactions between the positively charged lithium and negatively charged sulfur units of interacting polysulfide molecules, a cluster of polysulfides is found to be a more stable configuration compared to discrete, isolated polysulfide chains.^{30,32}

As shown in Figure 2, the formation energy sharply decreases with increasing cluster size, lowering by 18 kJ mol^{-1} as size is varied from 1 to 4 Li_2S_4 molecules. This reduction in energy appears to stabilize in clusters consisting of more than four Li_2S_4 subunits, as shown in Figure S2. In the limited kinetic energy environments that low temperatures present, this minimization of energy would likely drive equilibrium of lithium polysulfides towards highly clustered states at low temperatures. With increasing cluster size, there is geometrically a heightened degree of coordination and linking of strong $\text{Li}^+-\text{S}_4^{2-}$ partial bonds, which could prevent further lithiation and conversion. Thus, first-principles calculations strongly support that polysulfide clustering may be the dominant mechanism behind the low-temperature electrochemical behavior seen in Li-S batteries.

Experimental Confirmation of Polysulfide Clustering:

The bonding environment of a species of interest can be further evaluated via Nuclear Magnetic Resonance (NMR) spectroscopy, which evaluates the resonant frequency of each ion under an applied magnetic field. Thus, the low-temperature aggregating nature of polysulfides was investigated through studies with ^7Li -NMR spectroscopy, shown in Figure 3. Samples containing 0.1 M nominal Li_2S_4 in a 1:1 combination of DME and deuterated tetrahydrofuran (THF) solvent were analyzed at both room temperature and low temperatures of -60°C , with the resulting differences in peak location providing information on the change in ^7Li bonding environment in the sample.

At room temperature, a single peak corresponding to the $\text{Li}^+-\text{S}_x^{2-}$ bond environment is seen at 0.33 ppm, in relation to a LiCl reference dissolved in THF solvent. As the temperature is reduced to -60°C , however, the primary peak corresponding to this bond environment noticeably shifts upfield to 0.10 ppm, and further, a completely new peak emerges slightly downfield at 0.15 ppm. This behavior is strongly consistent with the suspected occurrence of

polysulfide clustering at low temperatures, as the shift upfield may be due to increased electron shielding.

The increased tendency of polysulfides to aggregate would be accompanied by the formation of a greater number of $\text{Li}^+\text{-S}_4^{2-}$ linkages. This increased degree of coordination with electron-rich sulfur atoms increases the local electron density in the vicinity of each lithium atom. This behavior is confirmed through a partial charge analysis detailed in Table S1. Therefore, in a clustered state, the average lithium atom likely experiences strong diamagnetic shielding from the greater surrounding electron density, resulting in a weaker effective field exposure and a shift upfield. The presence of an additional peak further supports this hypothesis, as there are a multitude of different Li-S bond environments with increasing polysulfide cluster complexity. Furthermore, lithium chemical exchange would drastically reduce between these clustered sites at low temperatures, resulting in observable peak splits.^{29,33} A variation of this experiment was performed on dissolved lithium salts in glyme-based solvents, and as shown in Supporting Information Figure S3, strong shifts are not observed at -60°C . This confirms that the observed shifts for Li_2S_4 are an intrinsic, species-related tendency to aggregate at low temperatures, and not just simply related to a temperature-dependent property of the solvent. This clustering behavior is further corroborated through studies using Fourier Transform Infrared (FTIR) spectroscopy, expanded upon in Figure S4 and the accompanying discussion. More broadly, this conclusion confirms an entirely new mechanistic insight into nonaqueous polysulfide solution chemistry.

The existence of large clustered aggregates of Li_2S_4 would present severe chemical, conformational, and electronic kinetic hurdles towards electrochemical lithiation and conversion. A greater minimization of formation energy at a stage stoichiometrically equivalent to Li_2S_4 would increase the already significant chemical activation barrier of the conversion to Li_2S crystallites. The expected reaction pathway would require the large aggregates to dissociate into individual polysulfide chains before further lithiation, an action that would be stifled by the robust electrostatic linkages holding the aggregate together. This activation barrier would be amplified by the severe steric barriers present in highly tangled and disordered aggregates, which could stifle the dissociation into individual polysulfide units. Large aggregates in solution would also hinder diffusion of polysulfides, which could further subdue the electrochemical reaction kinetics and affect the electrodeposited evolution of Li_2S .³⁴ Such a sign would be particularly noticeable in the second voltage plateau during electrochemical discharge, and consistent with our hypothesis, this is exactly what is seen in Li-S battery behavior at low temperatures.

Additionally, the favorable energetics of clustering phenomena suggest this behavior is present to a lesser extent even at room temperature, and may be an underlying cause of the poor electrochemical utilizations ($\sim 60\%$) generally seen in the broader Li-S battery literature.²¹ The variation in clustering phenomena tendency with temperature is expanded upon in Figure S5 and the accompanying discussion. The existence of these highly clustered states is fundamental to consider when developing strategies to implement this battery technology for target applications.

Interplay of Lithium Salt on Low-Temperature Solution Coordination:

In the Li-S electrolyte, lithium salt and lithium polysulfide coexist simultaneously in solution, and particularly in a limited electrolyte environment, their coordination states can influence and depend on each other in a dynamic, competitive equilibrium.²⁷ As shown through studies with FTIR spectroscopy, detailed in Figure S4 and the accompanying discussion, the coordination state of lithium salt and polysulfide in the electrolyte exhibit large dependencies on each other at low temperatures. This is due in large part to the dynamic electrostatic interactions occurring between species in solution.

A Li^+ cation in solution will be exposed to multiple electrostatic attraction forces from both the polysulfide and salt anion, and the end result of how the net interaction carries out can have a large impact in determining the coordination behavior each species.²⁹ If the lithium cation has greater overall tendency to coordinate with the polysulfide dianion than the salt anion, this will lead to more abundant $\text{Li}^+-\text{S}_x^{2-}$ bond network formation and subsequent polysulfide clustering. Conversely, increased attraction to the salt anion will lead to less abundant polysulfide clustering, as the $\text{Li}^+-\text{S}_x^{2-}$ bond network will not be as widespread. In this way, the deliberate use of competing lithium species in solution can be used to influence the nature of coordination and aggregation of lithium polysulfides. This interplay between competitive electrostatic interactions and coordination behavior of lithium species is illustrated in Figure 4.

Effective competitiveness of salt anions for Li^+ can be dramatically amplified by manipulating the electrolyte salt's physical properties, including both its ionic association strength as well as its concentration in solution.³⁵⁻³⁷ A lithium species' ionic association energy represents the anion's affinity for the Li^+ cation, which could determine the extent to which the compound participates in these competitive electrostatic interactions integral to Li-S solution behavior. The use of lithium salts engineered to be better competitors for lithium cations could be highly beneficial for use in low-temperature Li-S electrolytes. Their greater energetic attraction to Li^+ would be a stronger competing force that could more effectively weaken strongly bound $\text{Li}^+-\text{S}_x^{2-}$ networks, and possibly mitigate clustering phenomena. These energies were calculated and are shown in Table 1.

Lithium triflate (LiTF) possesses an ionic association energy of -74 kJ mol^{-1} , while the weakly bound lithium bis(trifluoromethane)sulfonimide (LiTFSI) exhibits an association energy of -58 kJ mol^{-1} . We propose the use of lithium trifluoroacetate (LiTFA) as the opposite extreme to LiTFSI, a strongly bound salt with association energy of -93 kJ mol^{-1} , in order to develop an optimized low-temperature Li-S electrolyte composition. This value approaches the energy for that of lithium polysulfide species, maximizing competitiveness for Li^+ cations, and ideally discouraging the formation of polysulfide clusters. Li-S cells were constructed with optimized electrolytes containing 85:15 (by volume) DOL:DME, 0.2 M LiNO_3 , and 0.7 M of either LiTFSI, LiTF, and LiTFA. The solvent ratio in these formulations was optimized for low temperatures in prior literature,⁹ as the increased DOL content likely minimizes variability in the coordination environment around solvated species as temperature decreases.^{31,38,39} These cells were cycled at a range of temperatures from 25 to -40°C (Figure S6), with representative electrochemical behavior at each temperature shown in Figure 5.

As can be seen, the use of LiTFA salt allows for substantial performance improvement over that with LiTFSI salt during sustained cycling at low temperatures. While LiTFA displays a sizeable 13% improvement at 0° C (Figure 5b), it shows a tremendous 167% capacity improvement over LiTFSI at -20° C (Figure 5c). Notably, there is a marked improvement in capacity extracted from the second voltage plateau. This indicates that the stronger binding LiTFA salt greatly mitigates polysulfide clustering phenomena and enables substantial conversion of Li_2S_4 to Li_2S . Similarly, the use of LiTF salt provides a large 120% capacity improvement over LiTFSI at -20° C, but does not outperform LiTFA, bolstering the trends demarcated from each compound's ionic association energy. Even more so, it does this with a large nucleation overpotential of 0.1 V, highlighting the severe kinetic limitations hindering this conversion at low temperatures. Furthermore, the poor performance of LiTF salt compared to LiTFSI at 0° C highlights a trade-off between conductivity and association energy. LiTF has neither greater conductivity than LiTFSI nor greater association energy than LiTFA, and thus fails to outperform either salt in any respect at 0° C. Only when clustering becomes a more critical problem, such as at -20° C, does the LiTF finally allow for better performance than LiTFSI. However, these performance improvements halt at -40° C. This is reasonable given that the clustering behavior is highly favored from an energetics consideration, and manipulation of salt to improve polysulfides coordination state can only mitigate, not prevent, the inevitable formation of polysulfide aggregates. The variability in performance from simply altering the lithium salt anion, which represent a single optimization in the overall parametric space, highlights the degree to which this system could be further enhanced for low-temperature conditions.

Conclusion

Here, we have identified and investigated polysulfide clustering as an emergent low-temperature phenomenon in Li-S batteries, and more broadly, have expanded the understanding of nonaqueous solution chemistry of lithium compounds. The poor kinetics of electrochemical conversion in large polysulfide clustered aggregates presents a key hurdle for the use of Li-S batteries at low temperatures and more broadly has significant implications for room-temperature behavior. Additionally, by investigating the mechanistic underpinnings of this system, we have identified clear design principles for significant optimization of low-temperature behavior. The use of strongly bound lithium salts such as LiTFA can tune the interdependent electrostatic interactions taking place within the electrolyte to discourage the onset of polysulfide clustering. This allows for significantly boosted conversion of Li_2S_4 to Li_2S at low temperatures, as the strongly binding TFA^- anion disrupts the robust $\text{Li}^+\text{-S}_4^{2-}$ aggregated network. This solution provides large improvements simply by modifying the lithium salt anion and represents just a first step towards a fully optimized low-temperature system. Implementation of functionalized and electrocatalytic host materials to the cathode can expand upon the understanding introduced here, both to minimize the degree of polysulfide aggregation in solution and enhance the kinetics of reduction.⁴⁰⁻⁴⁴ Low-temperature optimization of the lithium-metal anode also presents key opportunities,^{45,46} particularly by considering the influence of polysulfide coordination state on interfacial stability. With continued scientific insights and mechanism-driven optimization, the Li-S battery may one day reach its full capability as the battery of choice

for challenging, low-temperature environments. Ultimately, the mechanistic insight provided here critically links the solution conformation and charge-transfer behavior of dissolved species in electrochemical systems and expands upon the intricate, polysulfide-rich chemistry of the Li-S battery.

Supplementary Material

Refer to Web version on PubMed Central for supplementary material.

Acknowledgements

Support for this work through a NASA Space Technology Research Fellowship (NSTRF) under award number 80NSSC17K0089 is graciously acknowledged. Additionally, the authors thank Dr. Garret Blake for his assistance with collecting Li-NMR data.

References

- (1). Chung SH; Manthiram A Current Status and Future Prospects of Metal–Sulfur Batteries. *Adv. Mater* 2019, 31 (27).
- (2). Huang C-K; Sakamoto JS; Wolfenstine J; Surampudi S The Limits of Low-Temperature Performance of Li-Ion Cells. *J. Electrochem. Soc* 2000, 147 (8), 2893.
- (3). Wang CY; Zhang G; Ge S; Xu T; Ji Y; Yang XG; Leng Y Lithium-Ion Battery Structure That Self-Heats at Low Temperatures. *Nature* 2016, 529 (7587), 515–518. [PubMed: 26789253]
- (4). Halpert G; Frank H; Surampudi S Batteries and Fuel Cells in Space. *Electrochem. Soc. interface* 1999, 8 (3), 25–30.
- (5). Li Q; Lu D; Zheng J; Jiao S; Luo L; Wang CM; Xu K; Zhang JG; Xu W Li+-Desolvation Dictating Lithium-Ion Battery's Low-Temperature Performances. *ACS Appl. Mater. Interfaces* 2017, 9 (49), 42761–42768. [PubMed: 29148705]
- (6). Smart MC; Ratnakumar BV; Surampudi S Electrolytes for Low-Temperature Lithium Batteries Based on Ternary Mixtures of Aliphatic Carbonates. *J. Electrochem. Soc* 1999, 146 (2), 486.
- (7). Zhu G; Wen K; Lv W; Zhou X; Liang Y; Yang F; Chen Z; Zou M; Li J; Zhang Y; et al. Materials Insights into Low-Temperature Performances of Lithium-Ion Batteries. *J. Power Sources* 2015, 300, 29–40.
- (8). Xu K Nonaqueous Liquid Electrolytes for Lithium-Based Rechargeable Batteries. *Chem. Rev* 2004, 104 (10), 4303–4417. [PubMed: 15669157]
- (9). Mikhaylik YV; Akridge JR Low Temperature Performance of Li/S Batteries. *J. Electrochem. Soc* 2003, 150 (3), A306–A311.
- (10). Ryu H-S; Ahn H-J; Kim K-W; Ahn J-H; Cho K-K; Nam T-H; Kim J-U; Cho G-B Discharge Behavior of Lithium/Sulfur Cell with TEGDME Based Electrolyte at Low Temperature. *J. Power Sources* 2006, 163 (1), 201–206.
- (11). Yu SH; Huang X; Schwarz K; Huang R; Arias TA; Brock JD; Abruña HD Direct Visualization of Sulfur Cathodes: New Insights into Li-S Batteries via Operando X-Ray Based Methods. *Energy Environ. Sci* 2018, 11 (1), 202–210.
- (12). Samaniego B; Carla E; O'Neill L; Nestoridi M High Specific Energy Lithium Sulfur Cell for Space Application. *E3S Web Conf* 2017, 16, 08006.
- (13). Gupta A; Bhargav A; Manthiram A Highly Solvating Electrolytes for Lithium–Sulfur Batteries. *Adv. Energy Mater* 2018, 1803096.
- (14). Zhang SS Liquid Electrolyte Lithium/Sulfur Battery: Fundamental Chemistry, Problems, and Solutions. *J. Power Sources* 2013, 231, 153–162.
- (15). Shen C; Xie J; Zhang M; Andrei P; Hendrickson M; Plichta EJ; Zheng JP Understanding the Role of Lithium Polysulfide Solubility in Limiting Lithium-Sulfur Cell Capacity. *Electrochim. Acta* 2017, 248, 90–97.

- (16). Peng HJ; Huang JQ; Liu XY; Cheng XB; Xu WT; Zhao CZ; Wei F; Zhang Q Healing High-Loading Sulfur Electrodes with Unprecedented Long Cycling Life: Spatial Heterogeneity Control. *J. Am. Chem. Soc* 2017, 139 (25), 8458–8466. [PubMed: 28301151]
- (17). Kolosnitsyn VS; Karaseva EV; Seung DY; Cho MD Cycling a Sulfur Electrode in Mixed Electrolytes Based on Sulfolane: Effect of Ethers. *Russ. J. Electrochem* 2002, 38 (12), 1314–1318.
- (18). Zou Q; Lu Y-C Solvent-Dictated Lithium Sulfur Redox Reactions: An Operando UV–Vis Spectroscopic Study. *J. Phys. Chem. Lett* 2016, 7 (8), 1518–1525. [PubMed: 27050386]
- (19). Li Z; Zhou Y; Wang Y; Lu YC Solvent-Mediated Li₂S Electrodeposition: A Critical Manipulator in Lithium–Sulfur Batteries. *Adv. Energy Mater* 2019, 9 (1), 1802207.
- (20). Johnson L; Li C; Liu Z; Chen Y; Freunberger SA; Ashok PC; Praveen BB; Dholakia K; Tarascon J-M; Bruce PG The Role of LiO₂ Solubility in O₂ Reduction in Aprotic Solvents and Its Consequences for Li–O₂ Batteries. *Nat. Chem* 2014, 6 (12), 1091–1099. [PubMed: 25411888]
- (21). McCloskey BD Attainable Gravimetric and Volumetric Energy Density of Li–S and Li Ion Battery Cells with Solid Separator-Protected Li Metal Anodes. *J. Phys. Chem. Lett* 2015, 6 (22), 4581–4588. [PubMed: 26722800]
- (22). Frisch MJ; Trucks GW; Schlegel HB; Scuseria GE; Robb MA; Cheeseman JR; Scalmani G; Barone V; Mennucci B; Petersson GA; et al. Gaussian 09, Revision A.02. Gaussian, Inc.: Wallingford CT 2009.
- (23). Hanwell MD; Curtis DE; Lonie DC; Vandermeersch T; Zurek E; Hutchison GR Avogadro: An Advanced Semantic Chemical Editor, Visualization, and Analysis Platform. *J. Cheminform* 2012, 4 (1), 17. [PubMed: 22889332]
- (24). Glendening ED; Reed AE; Carpenter JE; Weinhold F NBO Version 3.1.
- (25). Chung S-H; Chang C-H; Manthiram A Progress on the Critical Parameters for Lithium-Sulfur Batteries to Be Practically Viable. *Adv. Funct. Mater* 2018, 28 (28), 1801188.
- (26). Cuisinier M; Hart C; Balasubramanian M; Garsuch A; Nazar LF Radical or Not Radical: Revisiting Lithium-Sulfur Electrochemistry in Nonaqueous Electrolytes. *Adv. Energy Mater* 2015, 5 (16), 1401801.
- (27). Dillard C; Singh A; Kalra V Polysulfide Speciation and Electrolyte Interactions in Lithium–Sulfur Batteries with in Situ Infrared Spectroelectrochemistry. *J. Phys. Chem. C* 2018, 122 (32), 18195–18203.
- (28). Henderson WA Glyme-Lithium Salt Phase Behavior. *J. Phys. Chem. B* 2006, 110 (26), 13177–13183. [PubMed: 16805630]
- (29). Rajput NN; Murugesan V; Shin Y; Han KS; Lau KC; Chen J; Liu J; Curtiss LA; Mueller KT; Persson KA Elucidating the Solvation Structure and Dynamics of Lithium Polysulfides Resulting from Competitive Salt and Solvent Interactions. *Chem. Mater* 2017, 29 (8), 3375–3379.
- (30). Partovi-Azar P; Kühne TD; Kaghazchi P Evidence for the Existence of Li₂S₂ Clusters in Lithium-Sulfur Batteries: Ab Initio Raman Spectroscopy Simulation. *Phys. Chem. Chem. Phys* 2015, 17 (34), 22009–22014. [PubMed: 26235886]
- (31). Andersen A; Rajput NN; Han KS; Pan H; Govind N; Persson KA; Mueller KT; Murugesan V Structure and Dynamics of Polysulfide Clusters in a Nonaqueous Solvent Mixture of 1,3-Dioxolane and 1,2-Dimethoxyethane. *Chem. Mater* 2019, 31 (7), 2308–2319.
- (32). Vijayakumar M; Govind N; Walter E; Burton SD; Shukla A; Devaraj A; Xiao J; Liu J; Wang C; Karim A; et al. Molecular Structure and Stability of Dissolved Lithium Polysulfide Species. *Phys. Chem. Chem. Phys* 2014, 16 (22), 10923–10932. [PubMed: 24770561]
- (33). ímal V; Št pánková H; Št pánek J Analysis of NMR Spectra in Case of Temperature-Dependent Chemical Exchange between Two Unequally Populated Sites. *Concepts Magn. Reson. Part A* 2011, 38A (3), 117–127.
- (34). Lang S-Y; Xiao R-J; Gu L; Guo Y-G; Wen R; Wan L-J Interfacial Mechanism in Lithium–Sulfur Batteries: How Salts Mediate the Structure Evolution and Dynamics. *J. Am. Chem. Soc* 2018, 140 (26), 8147–8155. [PubMed: 29883104]
- (35). Sun K; Li N; Su D; Gan H Electrolyte Concentration Effect on Sulfur Utilization of Li-S Batteries. *J. Electrochem. Soc* 2019, 166 (2), A50–A58.

- (36). Chu H; Noh H; Kim Y-J; Yuk S; Lee J-H; Lee J; Kwack H; Kim Y; Yang D-K; Kim H-T Achieving Three-Dimensional Lithium Sulfide Growth in Lithium-Sulfur Batteries Using High-Donor-Number Anions. *Nat. Commun* 2019, 10 (1), 188. [PubMed: 30643115]
- (37). Pan H; Wei X; Henderson WA; Shao Y; Chen J; Bhattacharya P; Xiao J; Liu J On the Way Toward Understanding Solution Chemistry of Lithium Polysulfides for High Energy Li-S Redox Flow Batteries. *Adv. Energy Mater* 2015, 5 (16), 1500113.
- (38). Peled E; Sternberg Y; Gorenshtein A; Lavi Y Lithium-Sulfur Battery: Evaluation of Dioxolane-Based Electrolytes. *J. Electrochem. Soc* 1989, 136 (6), 1621–1625.
- (39). Kamphaus EP; Balbuena PB First-Principles Investigation of Lithium Polysulfide Structure and Behavior in Solution. *J. Phys. Chem. C* 2017, 121 (39), 21105–21117.
- (40). Zhu S; Wang Y; Jiang J; Yan X; Sun D; Jin Y; Nan C; Munakata H; Kanamura K Good Low-Temperature Properties of Nitrogen-Enriched Porous Carbon as Sulfur Hosts for High-Performance Li-S Batteries. *ACS Appl. Mater. Interfaces* 2016, 8 (27), 17253–17259. [PubMed: 27320408]
- (41). Fan C-Y; Zheng Y-P; Zhang X-H; Shi Y-H; Liu S-Y; Wang H-C; Wu X-L; Sun H-Z; Zhang J-P High-Performance and Low-Temperature Lithium-Sulfur Batteries: Synergism of Thermodynamic and Kinetic Regulation. *Adv. Energy Mater* 2018, 8 (18), 1703638.
- (42). Deng DR; Xue F; Bai CD; Lei J; Yuan R; Zheng M. Sen; Dong QF Enhanced Adsorptions to Polysulfides on Graphene-Supported BN Nanosheets with Excellent Li-S Battery Performance in a Wide Temperature Range. *ACS Nano* 2018, 12 (11), 11120–11129. [PubMed: 30359514]
- (43). Zhong Y; Yin L; He P; Liu W; Wu Z; Wang H Surface Chemistry in Cobalt Phosphide-Stabilized Lithium–Sulfur Batteries. *J. Am. Chem. Soc* 2018, 140 (4), 1455–1459. [PubMed: 29309139]
- (44). He J; Manthiram A A Review on the Status and Challenges of Electrocatalysts in Lithium-Sulfur Batteries. *Energy Storage Mater* 2019, 20, 55–70.
- (45). Wang J; Huang W; Pei A; Li Y; Shi F; Yu X; Cui Y Improving Cyclability of Li Metal Batteries at Elevated Temperatures and Its Origin Revealed by Cryo-Electron Microscopy. *Nat. Energy* 2019.
- (46). Yang Y; Davies DM; Yin Y; Borodin O; Lee JZ; Fang C; Olguin M; Zhang Y; Sablina ES; Wang X; et al. High-Efficiency Lithium-Metal Anode Enabled by Liquefied Gas Electrolytes. *Joule* 2019, 3 (8), 1986–2000.

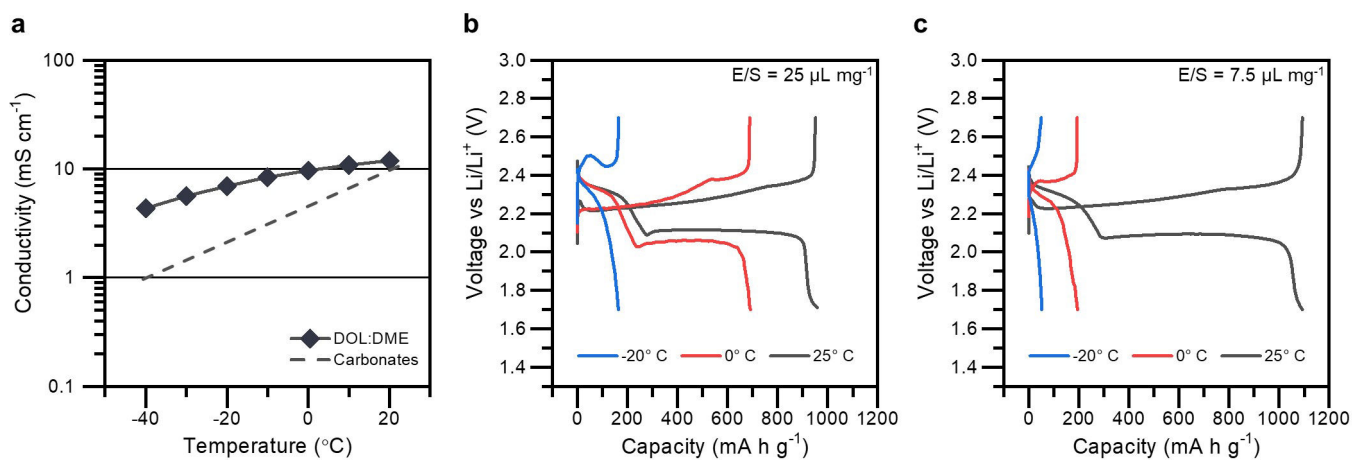


Figure 1.

(a) Loss in the conductivity of DOL-DME electrolyte from 20 to -40°C, in comparison to traditional carbonate electrolytes modelled from ref. 6. (b) Variation in the Li-S discharge and charge behaviors at 25, 0, and -20°C, in a cell with a large E/S ratio of 25 μL mg⁻¹. (c) Variable temperature performance of a Li-S cell with a lean E/S ratio of 7.5 μL mg⁻¹.

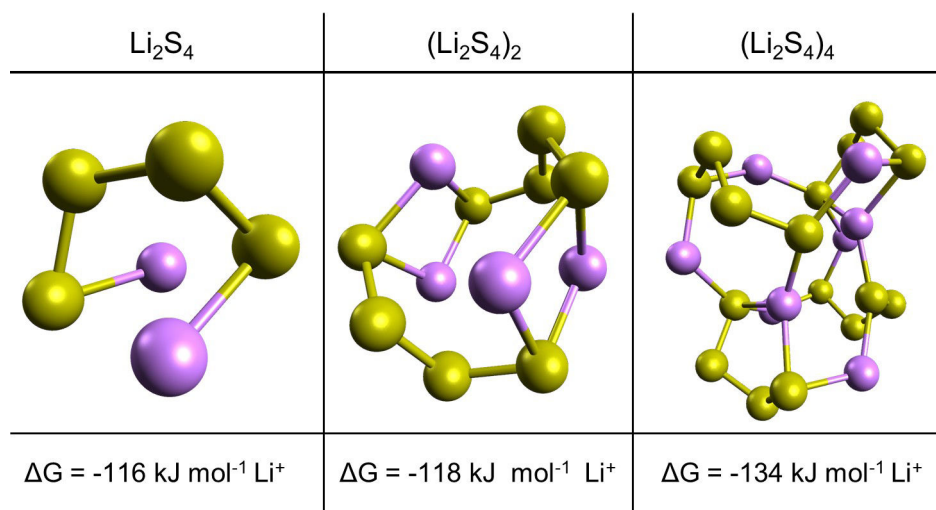


Figure 2. Computational evaluation of polysulfide clustering energetics, with the structures of various modelled $(\text{Li}_2\text{S}_4)_n$ clusters having size $n = 1, 2,$ and 4 . The accompanying formation energy of each cluster is shown on a $\text{kJ mol}^{-1} \text{ Li}^+$ basis.

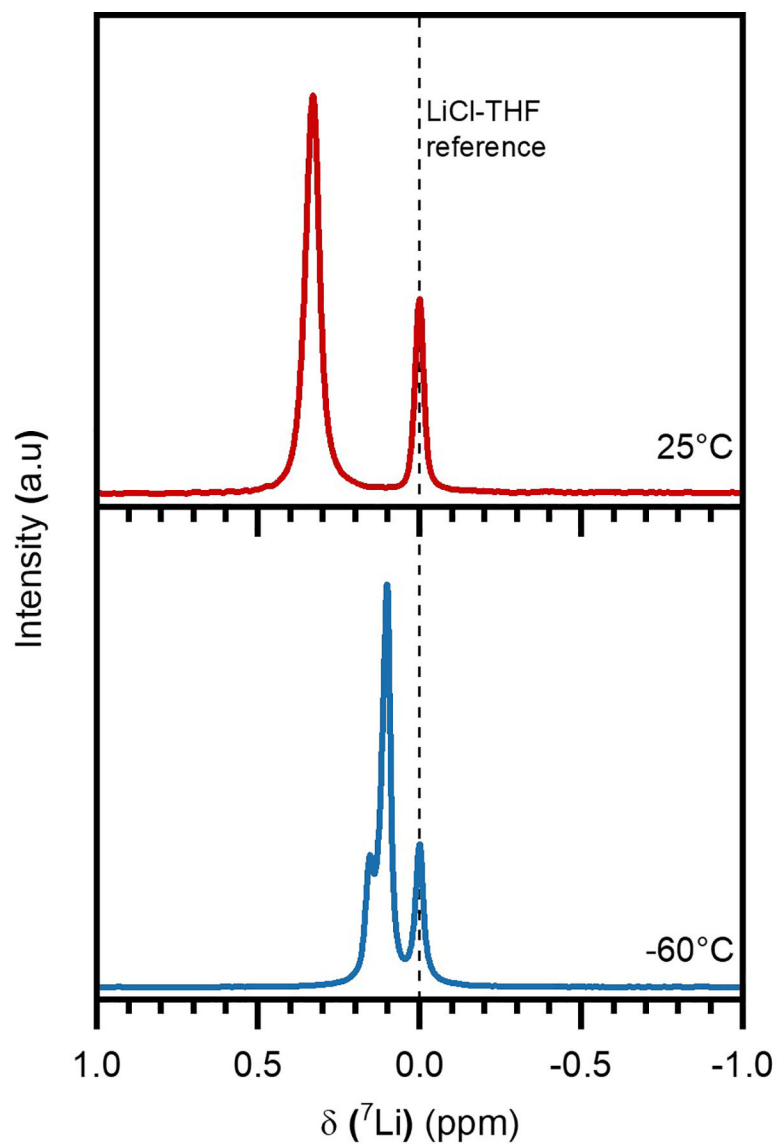


Figure 3. ${}^7\text{Li}$ -NMR performed on 0.1 M Li_2S_4 in d-THF:DME (1:1) at 25°C and -60°C, in relation to a LiCl reference (in THF) at 0 ppm.

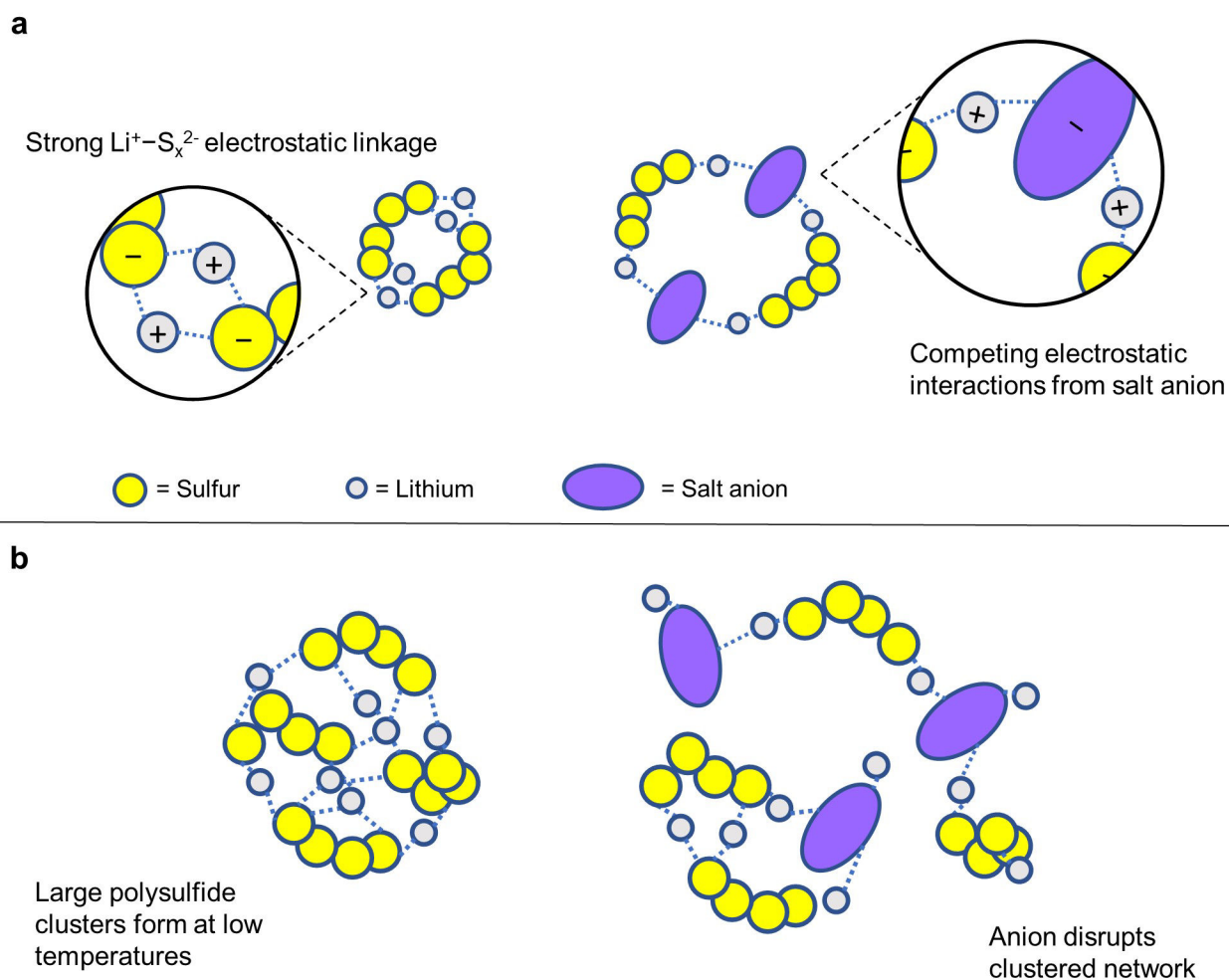


Figure 4. Illustration of competing interactions between lithium species in solution. (a) Strong $\text{Li}^+ - \text{S}_x^{2-}$ bond networks can be disrupted from competing electrostatic interactions between lithium ions and lithium salt anions. (b) The lithium polysulfides that naturally form at low temperatures can be disrupted from the influence of competing lithium salt.

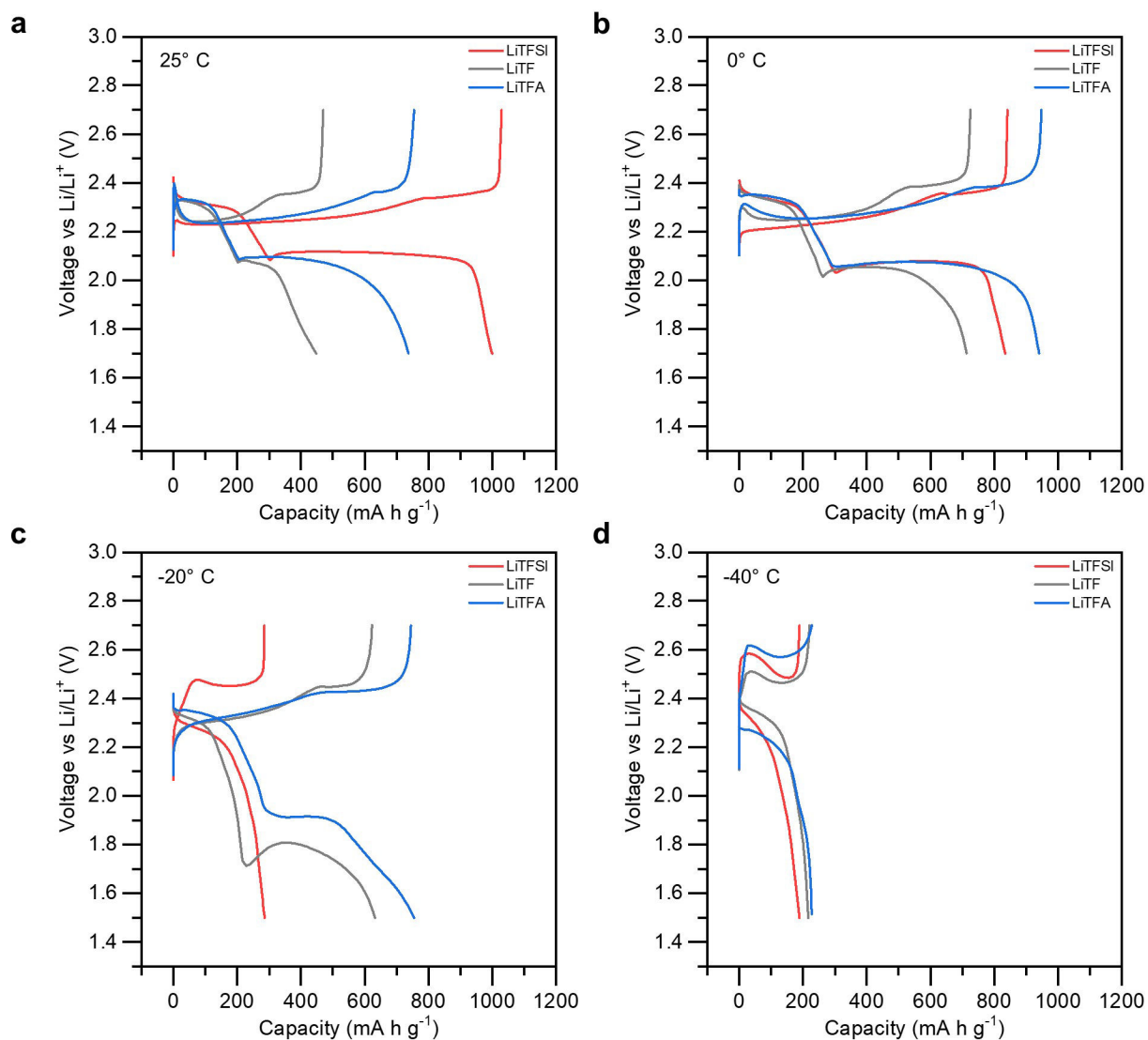


Figure 5. Variable temperature electrochemical behavior in Li-S cells utilizing LiTFSI, LiTF, and LiTFA salt, assessed at: (a) 25°, (b) 0° C, (c) -20° C, and (d) -40° C.

Table 1.

Calculated Ionic Association Energy of Various Lithium Salts and Polysulfide species

Species	$G_{\text{ion association}} \text{ (kJ mol}^{-1} \text{ Li}^{\text{+}}\text{)}$
LiTFSI	-58.11
LiTF	-73.94
LiTFA	-92.89
Li ₂ S ₄	-116.18
Li ₂ S ₆	-113.32
Li ₂ S ₈	-110.53